Available online at www.sciencedirect.com
SCIENCE DIRECT®
Journal of Nuclear Materials 323 (2003) 388–393
journal of nuclear materials
www.elsevier.com/locate/jnucmat

Irradiation induced behavior of pure Ni single crystal irradiated with high energy protons

Z. Yao *, R. Schäublin, M. Victoria

CRPP-EPFL Fusion Technology Materials, Villigen PSI 5232, Switzerland

Abstract

The microstructure and tensile behavior of pure single crystalline Ni irradiated to low doses at room temperature with 590 MeV protons are investigated. Tensile tests performed at room temperature show radiation induced hardening, which increases with increasing dose. The microstructure of irradiation induced defects observed under transmission electron microscopy consists of about 50% stacking fault tetrahedra, 30–40% dislocation loops and 10% of unidentified features. In addition, the irradiated and deformed specimen microstructure exhibits, at the beginning of deformation, shear bands as straight channels that are free of defects. The macroscopic results of the localized deformation have been observed during tensile test. The surface topography evolution is discussed in terms of localized shear and crystal rotation, which relates to the formation of deformation cells.

PACS: 61.72.Ff; 61.72.Ji; 61.72.Lk; 62.20.Fe

1. Introduction

The defect microstructure induced by irradiation in fcc pure metals has been extensively studied, in Cu, Ni, Pd and Au [1–5]. It is well accepted that a high density of defect clusters forms, that in the fcc lattice typically consist of stacking fault tetrahedra (SFT) and dislocation loops, resulting from the quenching and evolution of the displacement cascades.

In the case of the proton irradiated Cu at low temperatures, that is to say at about 0.2 T_m, where T_m is the melting temperature, it appears that SFTs dominate the irradiation induced defects in the displacement cascade regime [3,4]. The case of Ni, as one of the model fcc metals, is still not well understood. The experiments at low irradiation temperature, less than 0.3 T_m, from Zinkle and Snead [5] show a transition from a SFT-dominated microstructure at low doses to one dominated by interstitial dislocation loops at higher doses, with a threshold dose between 0.01 and 0.1 dpa. Earlier, Roberson et al. [6] reported 40% of SFTs in Ni irradiated with Ni^+ ions at RT to a dose estimated to be 0.001 dpa to 0.1dpa (10^{15}–10^{17} ions m^{-2}). It should be noted that this last irradiation was performed in situ in a thin foil TEM specimen, where surfaces may act as a sink for mobile dislocation loops.

Following this view, pure single crystal Ni irradiated at room temperature (about 0.2 T_m) with 590 MeV protons to a doses ranging from 0.001 dpa level to 0.1 dpa level is investigated.

Previously, Dai and Victoria [4] had systematically shown the irradiation effects in the proton irradiated Cu at low temperature. Irradiation hardening is present even at the lowest doses, down to 1×10^{-4} dpa. The activation volume analysis indicated that the initial plastic deformation was controlled by dislocation–irradiation induced defect interaction that then evolved into dislocation–dislocation interactions as the plastic deformation proceeds.

* Corresponding author. Tel.: +41-56 310 4538; fax: +41-56 310 4529.
E-mail address: zong-wen.yao@psi.ch (Z. Yao).

0022-3115/$ - see front matter © 2003 Elsevier B.V. All rights reserved.
doi:10.1016/j.jnucmat.2003.08.015

2. Experimental procedure

Single crystal rods of pure 99.999% nickel of 12 mm in diameter were provided by Goodfellow Cambridge Ltd. Plates 350 μm thick with the desired orientation were cut by spark erosion and tensile specimens of 2.5 mm gauge width and 5.5 mm gauge length with the Pirex geometry [7] were cut from the plates with a spark wire saw. The tensile orientation is close to (0 1 1), see Fig. 7(d). After mechanical polishing of the surfaces, the resulting thickness of specimen is about 300 μm, which is further reduced to about 250 μm after removing the work-hardened layer by electro-chemical polishing. All specimens were annealed in a high vacuum of about 10^{-5} mbar at 1273 K for 2 h followed by a slow cooling to room temperature.

The tensile specimens were irradiated at about 60 °C in the PIREX facility [8] installed in the 590 MeV proton beam of the accelerator located at the Paul Scherrer Institut in Switzerland. The typical dose rate is

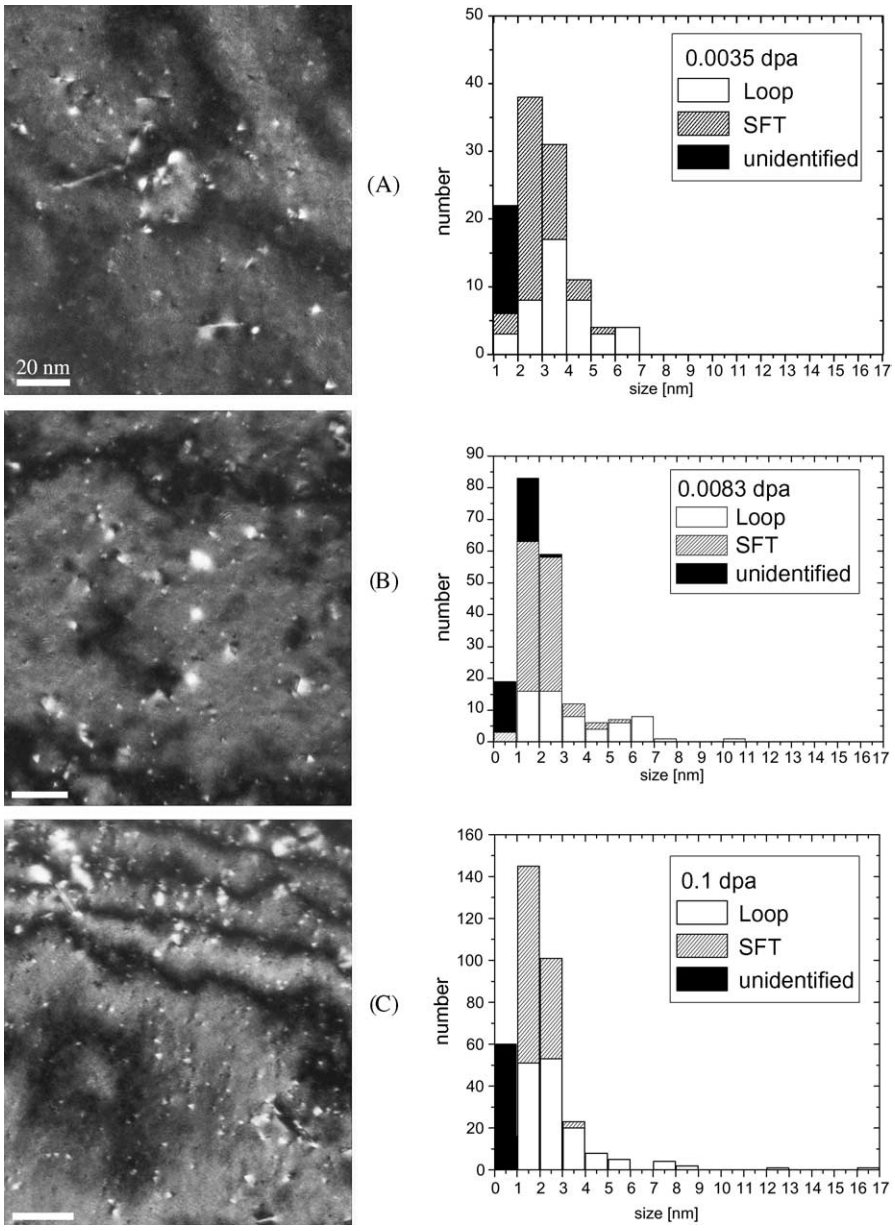

Fig. 1. Irradiation-induced defects in pure Ni and their size distribution, $\mathbf{g} = (200)$, weak beam g (5 g). (A) 3.5×10^{-3} dpa, (B) 8.3×10^{-3} dpa, (C) 1.0×10^{-1} dpa.

5×10^{-7} dpa s^{-1}. The tensile tests were performed at room temperature in air on a micro tensile testing machine. All tests were performed at a speed of 0.3 μm s^{-1}, corresponding to a nominal shear strain rate of about 5×10^{-5} s^{-1}.

TEM specimens of the unirradiated deformed specimen and of the irradiated and deformed ones were prepared. As Ni is magnetic, the volume of the TEM specimen was reduced by the following technique. First, discs with a diameter of 1 mm were punched and then concentrically glued into a stainless steel ring with an outer diameter of 3 mm. The composite specimens were first mechanically polished and then jet-electro-polished at 0 °C in a solution of 12% H_2SO_4 in methanol under 15 V. TEM examinations were performed in a JEOL 2010 operated at 200 kV.

A Zeiss DSM 932 operated at 30 kV was used for the SEM observations of the surface morphology of the tensile samples. A TV digital camera running at 25 frames per second was used for the in situ optical observation of the surface deformation during tensile testing.

3. Results and discussion

3.1. Microstructure of irradiation induced defects

Fig. 1(A)–(C) show the microstructure of the irradiation induced defects at three doses, which consists of loops and SFTs, together with their size distributions shown in right side. The observations were performed using TEM weak beam technique. The measured defects densities are 1.1×10^{23}, 2.4×10^{23} and 7.0×10^{23} m^{-3} for 3.5×10^{-3}, 8.3×10^{-3} and 1.0×10^{-1} dpa samples respectively. The density in the 1.0×10^{-1} dpa sample is much higher than that found in [7] at the same dose, 2.1×10^{23} m^{-3}. The reason for this difference is an improvement of experimental conditions, which resulted in a reduction of the oxide layer formed on the TEM samples' surface before observation.

The defect size distributions at different doses indicate that (i) the SFT represents 40–50% of the total defect density while the rest of the defects are loops, with 10–20% of unresolved small dots at all three doses as illustrated in Fig. 2, and (ii) the mean size of SFT's is independent of dose, which is about 2 nm and (iii) more loops with a large size, of over 10 nm, are present at 0.1 dpa than at 0.0083 dpa. Almost no large loops are observed at 0.0035 dpa.

3.2. Mechanical tests

The tensile response of single crystal Ni at the various irradiation doses is shown in Fig. 3, including the behaviour of the unirradiated material. It appears that

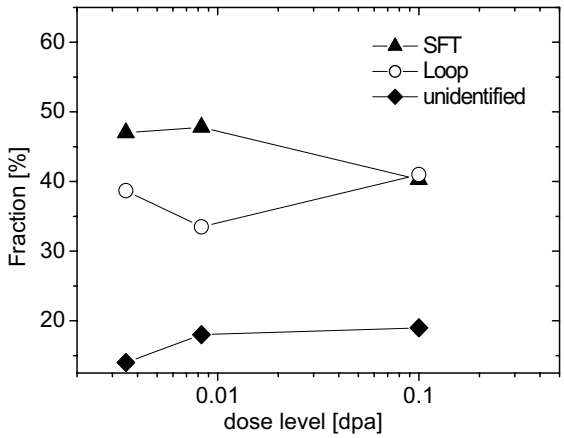

Fig. 2. The fractions of SFTs, loops and unidentified dots in irradiated samples at the different dose levels.

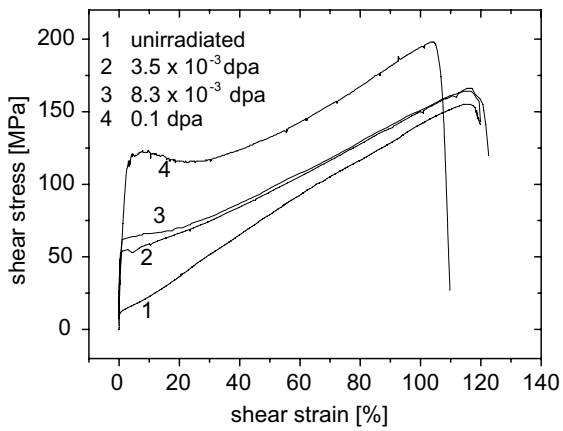

Fig. 3. The shear stress–shear strain curves of Ni single crystals, proton irradiated to different doses at room temperature. Irradiation doses (in dpa) are indicated on the stress–strain curves.

irradiation hardening is already present at the lowest dose. The critical resolved shear stress (CRSS) increases with increasing dose, as shown in Fig. 4. Stress serrations observed during the initial yield region have a larger amplitude and are more extended with increasing dose.

3.3. The activation volume

The activation volume is a measure of the volume of interaction of the dislocation with the obstacle and provides a good indication on the type of operating mechanism responsible for this interaction. The method used here for its measurement is that of successive stress relaxations at different stress levels along the tensile

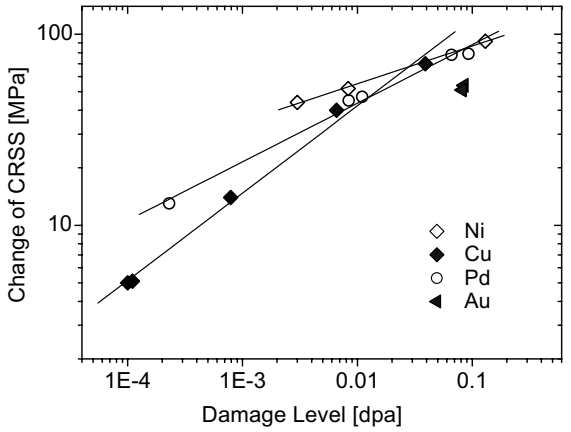

Fig. 4. Critical resolved shear stress (CRSS) as a function of irradiation doses.

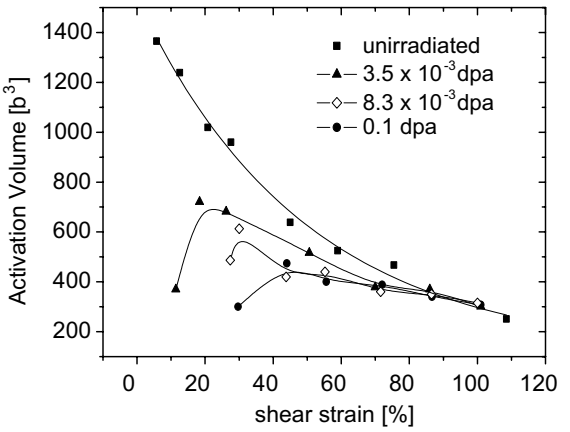

Fig. 5. Effective activation volumes for dislocation–defect interaction in Ni single crystals, deformed at RT.

curve [9]. The cross-head of the tensile machine is stopped for a given time and the stress drop $\Delta\tau$ is measured. The apparent activation volume V_a, on a single relaxation is given in this case by fitting the following relation: [10]

$$\Delta\tau = kT/V_a \ln(1 + t/c), \quad (1)$$

where c is an adjustable time constant, t is the relaxation time, T the test temperature, and k the Boltzmann constant. A correction for the strain hardening is calculated by performing successive relaxations in order to obtain the effective activation volume V_{eff} [9]. Measurements in the Ni single crystals are plotted as a function of the shear strain in Fig. 5. The relaxation stress drop ($\Delta\tau$) can be described as in [11]

$$\Delta\tau = \Delta\tau_d + \Delta\tau_f. \quad (2)$$

$\Delta\tau_d$ is due to the dislocation-irradiated induced defect interaction and $\Delta\tau_f$ is due to moving dislocation-forest dislocation interaction.

In the unirradiated case, $\Delta\tau_f$ dominates the relaxation process. Due to the initial very low density (10^{11}–10^{12} m^{-1}) of dislocations in the sample, the activation volume starts from a value of more than 1500 b^3 where b is the module of the Burgers vector. It then decreases rapidly, because of the dislocation density increases due to the deformation. Eventually the activation volume tends to a value around 300 b^3.

In the irradiated case, at the start of the deformation the main obstacles to dislocation movement are the radiation induced defects, with a mean distance of 50 nm between them. At higher dose the activation volume is even smaller, corresponding to the smaller mean distance between obstacles resulting from higher defect density. The activation volume increases and reaches a

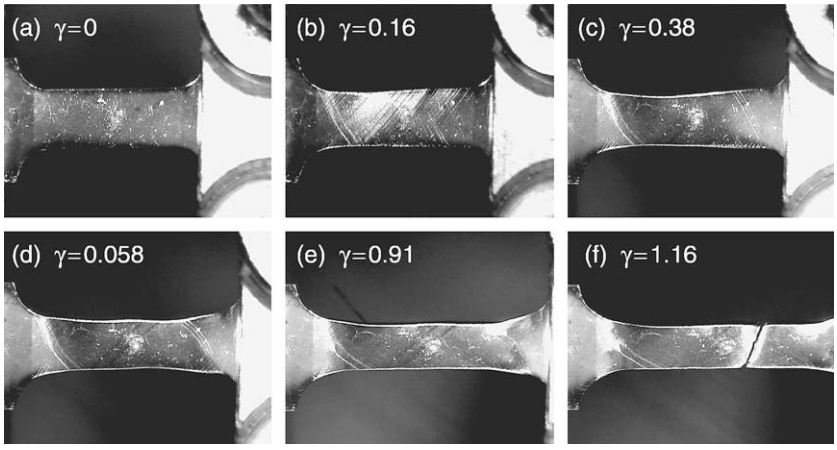

Fig. 6. Surface slip lines evolution in a Ni single crystal with a dose of 0.1 dpa.

peak value, as the deformation proceeds and the total density of obstacles decreases (their mean distance increases) through their interaction with dislocations and the formation of channels. Finally the interaction with other forest dislocations becomes the dominant mechanism as the mean distance between the radiation induced defects becomes comparable to that of forest dislocations. Deformation leads to a higher dislocation density, which consequently leads to a decrease in the activation volume down to similar values of 300 b^3 as in the unirradiated case.

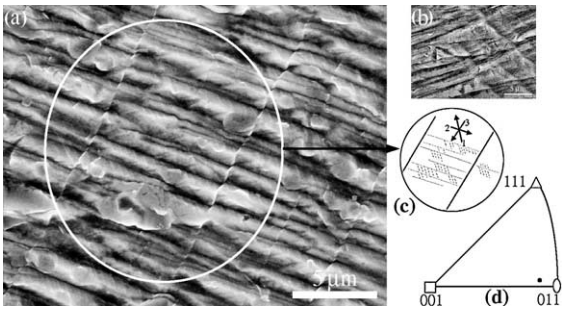

Fig. 7. (a) and (b) are the surface morphology of a region near the crack in irradiated and unirradiated case, respectively, (c) illustrates slipping traces of various gliding system and (d) shows the orientation of the sample crystal tensile axis.

3.4. The surface topography evolution in the tensile samples

Previous work [7] has shown that the main deformation mode in irradiated specimens is dislocations-free channelling. In what follows, the overall effects of this localized shear are investigated in the surface of the specimen. Fig. 6 shows the in situ observation by video camera of the surface slip bands evolution during a tensile test of an irradiated sample. As the earlier experiments showed [4,12], the slip band clusters appear as soon as the specimen yields and, later, spread over the whole gage length. Fig. 7(a) and (b) show the SEM observation in the region near the crack of both irradiated and unirradiated samples, respectively. Fig. 7(c) shows the replica drawing of the slip traces on the surface in Fig. 7(a). The numbers and arrows in Fig. 7(c) show the different slip systems. The first is primary slip system, the second is the conjugate slip system and the third is the cross-slip system. The mean distance between the primary slip bands in Fig. 7(c) is about 400 nm. Considering the orientation of the tensile axis shown in Fig. 7(d), this mean value corresponds to an actual distance of 700 nm, which is approximately equivalent to the mean spacing between channels in the microstructure of samples [7]. The analysis of the deformation at the surface is shown in Fig. 8(A)–(C). Fig. 8(A) shows the original surface of the tensile sample. The black marks from point ① to point ⑩ on the surface are used for analysing different sections along the gage length.

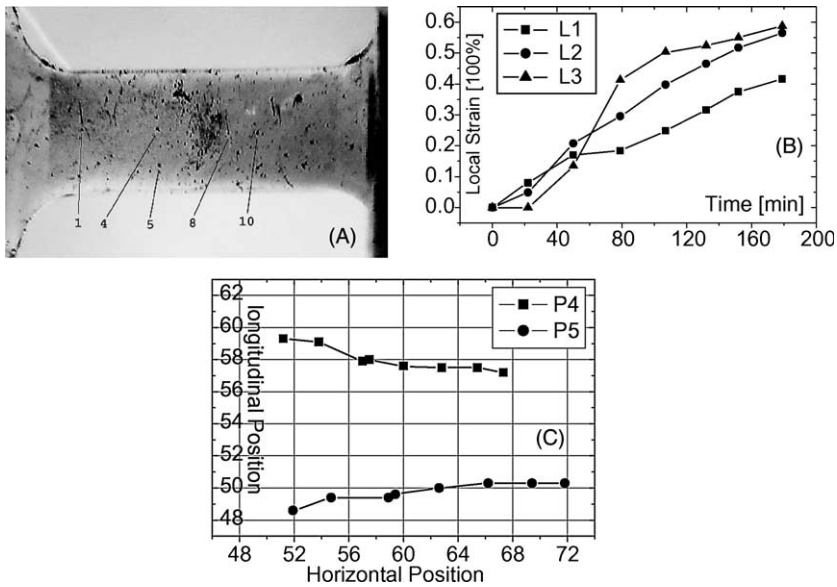

Fig. 8. (A) A few original points on the surface of sample are marked as reference for the measure of the local deformation. (B) shows the partial strain of three local lengths between point ①-point ④ (ΔL_1), point ④-point ⑧ (ΔL_2) and point ⑧-point ⑩ (ΔL_3). (C) shows the inhomogeneous migration of some points during tensile test.

The section ΔL_1 is taken from point ① to point ④, ΔL_2 from point ④ to point ⑧, and ΔL_3 from point ⑧ to point ⑩. Fig. 8(B) indicates these three sections in the gage length do not initially deform synchronically. The deformation is initiated almost only in the regions ΔL_1 and ΔL_2, and then only then in region ΔL_3, as confirmed by the surface slip traces. As in the sequence shown in Fig. 6(a)–(f) the deformation of the crystal indicates inhomogeneous and consequently localized in slip region. As the work hardening in the region ΔL_1 and ΔL_2 increases their deformation stress gradually, the region ΔL_3 starts to be deformed. After a shear strain is about 0.6, further deformation is almost linear and homogenous. Fig. 8(C) indicates the migration of point ④ and point ⑤ originally located approximately at the same X position. Following these moving traces, it can be concluded that a rotation also happened in the region ΔL_2 during the 34–53% of the tensile strain.

4. Conclusions

As a result of irradiation of Ni a high density of defect clusters is found. About 40–50% of clusters are SFTs while the rest are loops and unidentified small dots.

Starting at the lowest dose there is an increase of the yield stress with increasing dose.

Results indicate that in irradiated samples the main deformation mechanism changes from the breaking of irradiation induced defects to the cutting of the forest dislocations as deformation proceeds. The transition from one to the other is evidenced by the behavior of the effective activation volume.

The surface topography observation confirms that the plastic deformation in the slip region at the beginning of the tensile test of crystal proceeds localized and inhomogeneously.

Acknowledgements

Drs N Baluc, P Veyssière and P Spätig are thanked for their help and profitable discussions. PSI is acknowledged for the overall use of the facilities. This research is funded by contract No. 20-61837.00/1 of the Swiss National Science Foundation.

References

[1] M. Victoria, N. Baluc, C. Bailat, Y. Dai, M.I. Luppo, R. Schäublin, B.N. Singh, J. Nucl. Mater. 276 (2000) 114.
[2] M. Kiritani, T. Yoshiie, S. Kojima, Y. Satoh, K. Hamada, J. Nucl. Mater. 174 (1990) 327.
[3] B.N. Singh, S.J. Zinkle, J. Nucl. Mater. 206 (1993) 212.
[4] Y. Dai, M. Victoria, Mater. Res. Soc. Symp. Proc. 439 (1996) 319.
[5] S.J. Zinkle, L.L. Snead, J. Nucl. Mater. 225 (1995) 123.
[6] I.M. Robertson, J.S. Vetrano, M.A. Kirk, M.L. Jenkins, Philos. Mag. A 63 (1991) 299.
[7] Z. Yao, R. Schäublin, M. Victoria, J. Nucl. Mater. 307–311 (2002) 374.
[8] P. Marmy, M. Daum, D. Gavillet, S. Green, W.V. Green, F. Hegedus, S. Proennecke, U. Rohrer, U. Stiefel, M. Victoria, Nucl. Instrum. and Meth. B 47 (1990) 37.
[9] P. Spätig, J. Bonneville, J.-L. Martin, Mater. Sci. Eng. A 167 (1993) 73.
[10] F. Guiu, P.L. Pratt, Phys. Stat. Sol. 34 (1969) 9.
[11] Y. Dai, 1995, PhD thesis No 1388, École Polytechnique Fédérale de Lausanne.
[12] H. Neuhäuser, R. Rodloff, Acta. Meter. 22 (1974) 375.